Systematic reduction of a detailed atrial myocyte model

Daniel M. Lombardo and Wouter-Jan Rappel[a)]
Department of Physics, University of California, San Diego, California 92903, USA

(Received 5 December 2016; accepted 1 May 2017; published online 24 August 2017)

Cardiac arrhythmias are a major health concern and often involve poorly understood mechanisms. Mathematical modeling is able to provide insights into these mechanisms which might result in better treatment options. A key element of this modeling is a description of the electrophysiological properties of cardiac cells. A number of electrophysiological models have been developed, ranging from highly detailed and complex models, containing numerous parameters and variables, to simplified models in which variables and parameters no longer directly correspond to electrophysiological quantities. In this study, we present a systematic reduction of the complexity of the detailed model of Koivumaki *et al.* using the recently developed manifold boundary approximation method. We reduce the original model, containing 42 variables and 37 parameters, to a model with only 11 variables and 5 parameters and show that this reduced model can accurately reproduce the action potential shape and restitution curve of the original model. The reduced model contains only five currents and all variables and parameters can be directly linked to electrophysiological quantities. Due to its reduction in complexity, simulation times of our model are decreased more than three-fold. Furthermore, fitting the reduced model to clinical data is much more efficient, a potentially important step towards patient-specific modeling. *Published by AIP Publishing.* [http://dx.doi.org/10.1063/1.4999611]

Mathematical models are an essential tool for studying and understanding mechanisms of cardiac rhythm disorders. Of particular interest in this paper are the electrophysiological models that have been developed to study the membrane potential and ionic currents in heart cells. Many of these models can be extremely complex, making it difficult to extract pertinent information from them. Here, we examine a detailed model and show that it can be greatly reduced to a handful of equations that are needed to describe the membrane potential. Our simplified model is unique in that we started from a detailed, physiologically accurate model, so the parameters of the final model maintain their physiological significance.

INTRODUCTION

Atrial fibrillation (AF) is the most common cardiac arrhythmia and affects 2%–3% of the population in Europe and North America.[33] During AF, the heart rate becomes irregular, resulting in rapid and less efficient beating. AF is difficult to eliminate,[3,13] and the underlying mechanisms remain poorly understood. This incomplete understanding is mainly due to the difficulty in obtaining clinical data that quantify the spatio-temporal dynamics during AF. Based on animal data[9,10] and on recent recordings of human AF using basket electrodes[21–23] and high density body surface electrodes[12] it is believed, however, that spiral waves play a crucial role in the maintenance of human AF. Understanding how these spiral waves form and how they are responsible for the various clinical signatures of AF can potentially result in better treatment options for this serious disease.

Mathematical models can play an important role in improving treatment for cardiac diseases, including AF.[14] Simulations of single cells, tissue sheets, or the entire heart can provide useful insights into the role of different cell or tissue properties in cardiac arrhythmias.[4,25,26,31] A crucial component in these studies is the electrophysiological model that describes the voltage dynamics of a cardiac myocyte. This model consists of a set of coupled differential equations that characterize the ion channels within the cell and the resulting currents. A variety of models exist to characterize the excitation of a myocyte, known as an action potential (AP). These models vary in detail and the overall structure and can, along with the ionic channels, also include ionic concentrations inside the cell.

Recent studies aim to improve upon the accuracy and capabilities of previous models,[5,8,19] such as adding a component to characterize the role of the sarcoplasmic reticulum. This results in increasing detail and complexity as the models add new equations and parameters to further describe electrophysiological properties of the cell. There are, however, several drawbacks of this added complexity. Obviously, adding equations and parameters comes at the expense of increased computational costs. Furthermore, whether this added complexity leads to improved accuracy is questionable since many channel properties are not well characterized or only measured using animal models. In addition, there is a large cell-to-cell variability within the heart and between different hearts, necessitating different and variable parameter sets. Thus, developing patient specific modeling, a goal of many current modeling studies,[20,29] would require extensive fitting to patient data. This fitting, however, is generally more difficult to accomplish in detailed models.[27] In a recent study, for example, we were able to fit a detailed cardiac model, the Koivumaki Korhonen Tavi (KKT) model,[16] to several clinical

a)Author to whom correspondence should be addressed: rappel@physics.ucsd.edu

data sets describing the action potential shape, action potential duration restitution, and conduction velocity restitution simultaneously. However, this came with a large computational cost.[18]

As an alternative to these detailed models, simplified descriptions of cardiac cells have been developed.[6,15,24] These models are computationally efficient, more intuitive to interpret, and their parameters can be adjusted to reproduce a large variety of spatio-temporal dynamics.[7] These models, however, characterize only a few key components that do not explicitly represent ion channels. Therefore, their parameters cannot directly be compared to physiologically relevant quantities such as ion channels.

It would therefore be useful to have a model that is simple, needing only a handful of differential equations, while still maintaining parameters that are related to physiological quantities. With this goal in mind, we carry out a reduction study of a detailed cardiac model using the Manifold Boundary Approximation Method (MBAM).[28] This method is particularly well-suited to reduce the number of parameters in the so-called "sloppy" models: models in which many parameters are loosely constrained and which only depend a few "stiff" parameter combinations.[2] It turns out that many system biology models exhibit sloppiness, which is also characterized by parameter sensitivity eigenvalues that are evenly distributed over many decades.[11] MBAM uses a geometric and information theoretic approach that can systematically reduce a model in a stepwise fashion.[28]

We will focus here on the highly complex and detailed KKT model[16] and carry out a stepwise reduction of parameters and variables using MBAM. We report results on 5 reduced models: 4 corresponding to intermediate reduction steps and one representing the final reduction. We show that these models are able to reproduce the AP shape, and AP restitution curve, linking the AP duration and the stimulus period, of the original model. The final reduction model has significantly fewer parameters and variables than the original one and has a significantly shorter computational time. Thus, its complexity is vastly reduced and approaches that of simplified models, without sacrificing the electrophysiological connection of the remaining model parameters and variables.

METHODS

As our electrophysiological model, we will use the KKT model of human atrial myocytes.[16] The KKT model was designed to characterize a wide range of quantities, including intracellular concentrations and calcium release from the sarcoplasmic reticulum. Several versions of the model are also presented in the original paper, with variations in complexity and results. Here, we use the vNassIk version of the model, with some modification.[17] In this version, a subsarcolemmal sodium concentration is added to the cell, along with a hyperpolarization activated potassium current. The model is comprised of 42 differential equations, with over one hundred possible parameters.

In terms of measured quantities, we only look at the action potential produced by the model, not the individual currents or concentrations. Simulations were run using an S1-S2 protocol. Meaning that a stimulus (S1) is applied repeatedly at a set cycle length for a given time duration, and then followed by a single stimulus (S2) at a different cycle length. After the single S2 stimuli, the pacing reverts back to the S1 stimuli and the process repeats. For our simulations, the S1 stimulus always had a 500 ms cycle length, and 5 S1 stimuli are applied in between each S2 stimuli. Three different S2 stimuli were used in the simulation, and were chosen to capture the general shape of the action potential duration (APD) restitution curve and to characterize tissue dynamics for both large and small cycle lengths. The action potential shapes generated from the three different S2 stimuli were recorded. This protocol is different from what is described in the original paper, which used several different pacing protocol, some running for several minutes, to quantify a variety of characteristics in the action potential shape and duration. These long simulation time scales would not be practical with the MBAM method, which requires many repeated simulations per reduction step.

Of the many parameters in the model, the time constants and the parameters that represented the extracellular concentrations and physical dimensions of the cell were kept fixed. The remaining parameters, containing all the model conductances, diffusion constants, buffer concentrations, and reaction rates, were allowed to vary in MBAM. For the version of KKT chosen here, this equates to a model with 42 variables and 37 parameters. Before beginning the reduction algorithm, all the parameters were first log transformed, $\bar{u} = \log(u)$, so that each parameter in the model reduction algorithm can vary between $\pm\infty$. This improves the accuracy of the algorithm, as it increases the range of variability for each parameter and makes them dimensionless quantities.

The MBAM reduction algorithm, further detailed in the Supporting Material, begins by creating a metric tensor of the parameter space manifold.[28] This is done by looking at a set of measured quantities produced by the model (see below), and examining how sensitive these are to changes in the parameter space. More precisely, the metric tensor is the Fisher Information Matrix. The eigenvalues of the metric then give a hierarchy of widths that characterize the parameter space. By moving along parameter space towards the nearest boundary, or shortest width, the dimensionality of the parameter space can be reduced. Furthermore, in order to ensure a minimal change in the results, the model advances towards the boundary along the geodesic lines of the manifold.

Sixty time points, twenty from each of the three S2 stimuli, were chosen in total for the data points, or measured quantities, in the reduction algorithm. These points were not evenly spaced along the voltage trace, but rather chosen to include values from the upstroke, repolarization, and resting state of the model (see Fig. S1 of supplementary material). At the end of each run of the reduction algorithm, the model was evaluated at the limit. This corresponds to setting the parameter(s) that will be removed to either 0, resulting in the elimination of a variable or a term in one of the equations, or ∞, which resulted in a fraction that vanishes. After the reduction step, the new and reduced model was refit to the output of the original model at the same sixty time points mentioned above using a simulated annealing method as

described in our earlier work.[18] The reduced model, along with its new parameters, was then used as input to the MBAM algorithm. This process was repeated until the reduced model could no longer be fit to the original model without significant error, defined as $> 10\%$ in the AP shape (see below).

All matrix manipulation required by the MBAM method was run on a Tesla K40 GPU using the CUDA parallel computing framework. Model simulations were run in serial on a quad-core Xeon E5-2637 CPU. A forward Euler scheme with a time step of 0.01 ms was used for the model simulations, and a variable time step was used for integrating the geodesic equation. Each successive step of the algorithm took less time to complete, as the model was reduced in complexity.

Accuracy of the fit was defined through an error function E which measures the discrepancy of the numerical results and the original KKT data as reported earlier[18]

$$E = \frac{1}{M}\sum_{i=1}^{M}\frac{|x_i^{sim} - x_i^{KKT}|}{|x_i^{KKT}|}, \tag{1}$$

where x_i^{sim} and x_i^{KKT} are the values of the simulation of the reduced and original model, respectively, and where M is the total points that are used in the error function.

RESULTS

We first determined the parameter sensitivity spectrum of the KKT model. To this end, we first computed the cost function, C, for the change in voltage, V, when parameters deviate from their original values. We use $M = 60$ time points t_m

$$C = \sum_{m=1}^{M}\frac{1}{2}\left(V(\vec{\theta}, t_m) - V\left(\vec{\theta}^{*}, t_m\right)\right)^2. \tag{2}$$

Here, $\vec{\theta}$ is a vector representing the set of all parameters. We then computed the eigenvalues of the Hessian matrix[11]

$$H_{i,j} = \partial_i \partial_j C. \tag{3}$$

Details of this calculation can be found in the supplementary material. The spectrum is plotted in Fig. 1 and spans roughly 20 orders of magnitude, with eigenvalues that are approximately equally spaced. The latter means that it is not possible to divide parameters into an important and a not so important group.

We next carried out a stepwise reduction of the KKT model with MBAM, and were able to reduce it from 42 variables with 37 parameters to only 11 variables with 5 parameters. In Fig. 2, we give a visual representation of four intermediate steps along with the final step, showing which parameters are removed after each reduction step. Henceforth, we will refer to these steps as R_1, R_2, R_3, R_4, and R_{final}. A similar figure of the change in variables is in Fig. S2 (supplementary material), and a list of the parameter values for each reduction step is in Table S1 (supplementary material).

In this representation, we have marked all parameters that were eliminated in red while the parameters in blue were combined into new parameters. As indicated in Fig. 2, the red parameters were eliminated in one of two ways. Some parameters, e.g., the conductance of the slow delayed rectifier potassium current, gKs, were set equal to 0, resulting in the complete removal of a current or equation term (Iks in our example). Other parameters appear in the denominator of the current equations and were set equal to ∞. Obviously, this also resulted in the elimination of these terms, together with parameters that appear in the numerator of these equations. These parameter combinations are marked by the bracket and an example is the concentration of the calcium buffer calsequestrin, CSQN, together with its dissociation constant KdCSQN. The parameters marked in blue appear in combinations that can be combined into a single parameter.

FIG. 1. Eigenvalue spectrum of the Hessian matrix for the original model and the final reduced model.

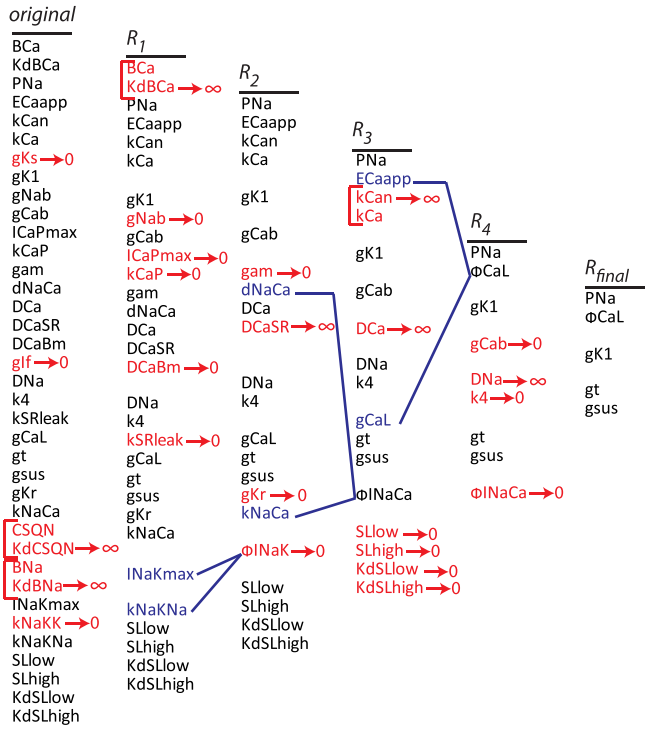

FIG. 2. Chart of parameter changes between iterations of the reduction algorithm. The parameters highlighted in red are ones that were removed in the following iteration, after being evaluated at a limit. The parameters highlighted in blue were reduced or combined to make new parameters.

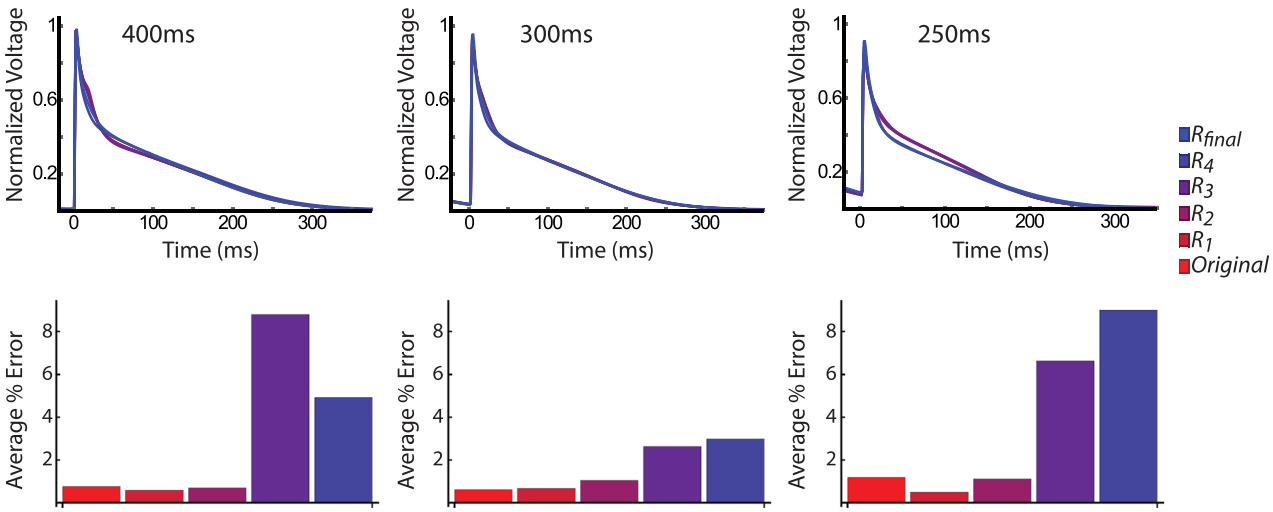

FIG. 3. AP Shape comparison for select iterations of the reduced model. The AP shape is shown for each of the S2 stimuli in the S1-S2 pacing protocol used in the reduction algorithm. The cycle lengths shown are 400, 300, and 250 ms. For clarity, the bar graph next to each curve shows the percent error in each of the models.

For example, when going to a boundary of the manifold, both INaKmax, the maximum value of the INaK current, and kNaKNa, the half maximum sodium binding concentration, were observed to grow quickly. Since these parameters are in the numerator and denominator, respectively, they can be combined into a new, and single one ϕ_{INaK}.

The final model contains only 5 parameters, representing the conductances of the 5 remaining currents: the fast sodium current I_{Na}, the L-type Ca2+ current I_{CaL}, the time-independent potassium current I_{K1}, the transient outward potassium current I_t current, and the sustained outward potassium current I_{sus}. These currents are unmodified from the original model, except the L-type calcium current which now depends on the parameter ϕ_{CaL}, which is the product of the original conductance and effective reversal potential (see supplemental material, where we also show for completeness the unmodified currents). The eigenvalue spectrum of the final reduced model R_{final} is shown in Fig. 1 and shows that the range has significantly decreased from the original model and now only spans 10^4.

We next determined how accurately the reduced models can reproduce the original model results. To this end, we fitted, after each reduction step, the remaining parameters of the model to the data as described in Methods. In Fig. 3, we plot the computed AP shape for all three S2 stimuli for the 4 intermediate steps and the final reduction step. As can be seen from these graphs, the AP shape remains close to the original one for all reduction steps. This can be quantified by computing the error between the original and the simulated AP curves (see Methods). The results are shown as bar graphs in Fig. 3 and demonstrate that this error remains $<2\%$ for R_1, R_2, and R_3 and becomes at most $\approx 8\%$ for R_4 and R_{final}.

To further quantify the outcomes of the reduction steps, we computed the APD restitution curve for our three S2 values. The results are plotted in Fig. 4 using the same color scheme as in Fig. 2. As expected, the restitution curves for all reduction steps are similar to the one from the original model. In Fig. S3 (supplementary material), we have plotted APD restitution curves for a larger range of S2 stimuli, showing identical qualitative behavior.

Attempting to proceed after R_{final} resulted in either the conductance of I_{K1} or of I_{sus} to go to 0. Fitting the resulting AP shape with these currents removed resulted in an error that was larger than 10% and the reduction process was stopped. We have also examined the stability of the action potential duration for each of the models, a desirable feature for cardiac simulations.[32] We found that the original model and the final model are roughly identical in their stability (see Fig. S4 of supplementary material), while the drift from the initial values was more pronounced in the intermediate models. The fact that the intermediate models show a more significant drift in voltage is perhaps not surprising. The resting potential is a result of a delicate balance between all currents, pumps, and exchangers. Removing some of these might result in a resting potential that slowly changes over time. Furthermore, even the original model shows a small drift. It also likely that constraining parameter values or further fitting with more data points can improve the stability of the reduced models.

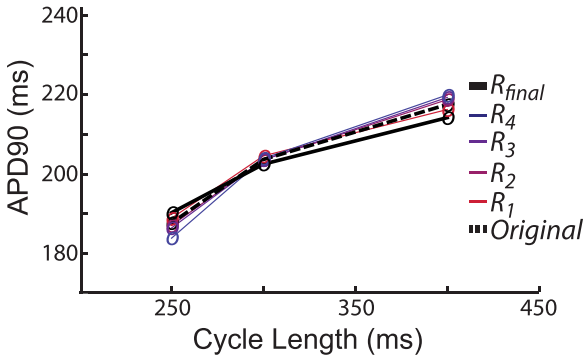

FIG. 4. APD Restitution curve for the original and reduced models. The APD was recorded from simulations using 3 S2 stimuli, as in the reduction/fitting process. The original and R_{final} models are represented as thick black lines, with the original also being dashed.

DISCUSSION

In this study, we systematically reduced a detailed model for atrial myocytes, containing many parameters and variables, to a relatively simple model with only 5 parameters and 11 variables. The reduction was carried out with MBAM, a geometric and information theoretic technique particularly well-suited for sloppy models. This sloppiness is manifested in the insensitivity of the model results to large parameter variations, as shown in the large and roughly even spread of eigenvalues (Fig. 1). Therefore, the model is only sensitive to a limited set of parameter combinations and should be amenable to parameter reduction.

Many of the currents in the original model were completely removed in the final reduced version. Perhaps this is not a surprise when one takes into account the result from previous studies. In the original publication of the KKT model,[16] it was reported that the addition of the hyperpolarization activated current I_f was added to the model but that it only has a small effect on the overall dynamics, as it only activates at hyperpolarized voltages compared to the resting (diastolic) potential. It is also stated that the I_{Ks} and I_{Kr} currents in the model should have a smaller effect than the I_{K1} current in determining repolarization. In agreement with this, our method removes the I_f, I_{Kr}, and I_{Ks} currents entirely, while keeping the I_{K1} current. Furthermore, Nygren *et al.* showed that the I_{CaP}, I_{Nab}, I_{Cab}, I_{NaK}, and I_{NaCa} currents are more relevant for maintaining sodium and calcium concentrations within the cell and do not change the response of the cell to a stimulus in a significant way.[24] As the goal of our reduced model was to characterize the action potential, it is reasonable that currents related to the ionic concentrations could be removed. Clearly, since our final reduced model does not explicitly solve for these concentrations, nor for the calcium concentration within the sarcoplasmic reticulum, it will not be able to address dynamics changes of these concentrations. We should point out, however, that some of these variables are still present in one of the intermediate models, which could be used instead. Furthermore, our reduction method focused on the voltage dynamics, using an S1S2 stimulus protocol. Reduction attempts that focus on the dynamics of some of the intracellular components might result in reduced models that maintain the ability to investigate the ionic concentrations.

Our final model resulted in AP changes and restitution curves that are close to the ones generated by the original model even though it contains many fewer variables and parameters. This suggests that our reduced model can be used as a viable alternative to the complex full model for the investigation of both single cell responses to different stimuli, and for the study of spatio-temporal dynamics in spatially extended geometries. As a simple example, we performed a 2D simulation in which we initiated spiral waves using a premature stimulus[1] (see Fig. S5 of supplementary material). The observed dynamics in the reduced model is qualitatively similar to the original model, albeit with a slightly lower conduction velocity. Consistent with the development of the original model, our reduced model excluded any selection for the conduction velocity, so it is to be expected that the simulations over extended domains contain some differences.

When trying to further reduce the model by eliminating one of the remaining 5 currents, the error in the resulting and the original AP shape became quite large. This suggests that using the ionic formulation of the KKT model it is not possible to accurately describe AP shapes without an explicit description of I_{Na}, I_{CaL}, I_{K1}, I_t, and I_{sus} and that our reduced model can be seen as a minimal atrial myocyte model. This does not mean that it is impossible to fit AP shapes with fewer variables, as, for example, in the Fenton-Karma model.[6] This model, however, does not utilize the same functional form for its variable equations which can no longer be directly equated to ionic currents.

While many of the components of the original KKT model were removed, this approach has also allowed for much of the detail and complexity to remain in the five currents that were kept in the model. Of these currents, only the L-type calcium channel was altered, and a physical description can still be associated with many of the parameters and variables. This is in contrast to the simple models that have been developed in the past. Not surprisingly, our reduced model is computationally more efficient than the original one. An estimate of the simulation times for the original and for the final model shows that the reduction resulted in an approximately three-fold speed-up: simulations of 1000 s for a single cell took 11.9, 11.1, 9.7, 8.6, 6.6, and 3.7 s for the original, R_1, R_2, R_3, R_4, and R_{final} models, respectively. We have verified that similarly a speed up can be seen when fitting the model to data, a task that is necessary for the development of patient-specific models.

CONCLUSION

Here, we showed how MBAM can systematically reduce the complexity of a detailed atrial model. Although we have focused here on a model for atrial myocytes, our reduction methodology can also be applied to models for ventricular myocytes.[30] The models presented here are capable of reproducing action potential dynamics that are equivalent, or nearly equivalent, to those produced by more detailed models. The approach used in this paper begins with a very complex model and successively removes all components which did not greatly affect the action potential or the APD. Meaning that only variables and parameters which have the greatest sensitivity to the measured quantities remain. Plus, this produces a series of increasingly simple models, instead of a single end result. From the final reduced model, we find that I_{K1}, I_{sus}, I_t, I_{Na}, and I_{CaL} currents are most relevant for determining the AP shape and duration. We conclude here that if one does need to study all the intricacies of intracellular concentrations, then a detailed model containing such components is not necessary for studying many of the remaining dynamics.

SUPPLEMENTARY MATERIAL

See supplementary material for further details of the MBAM method, and structure of the reduced models.

ACKNOWLEDGMENTS

We would like to thank Dr. Transtrum for helpful comments on the manuscript. We gratefully acknowledge the support of NVIDIA Corporation with the donation of the Tesla K40 GPU used for part of this research. This work was supported by National Institutes of Health R01 HL122384.

[1]R. R. Aliev and A. V. Panfilov, Chaos, Solitons Fractals **7**, 293 (1996).
[2]K. S. Brown and J. P. Sethna, Phys. Rev. E **68**, 021904 (2003).
[3]S. S. Chugh, R. Havmoeller, K. Narayanan, D. Singh, M. Rienstra, E. J. Benjamin, R. F. Gillum, Y.-H. Kim, J. H. McAnulty, Z.-J. Zheng *et al.*, Circulation **129**(8), 837–847 (2014).
[4]R. H. Clayton, A. Bailey, V. N. Biktashev, and A. V. Holden, J. Theor. Biol. **208**, 215 (2001).
[5]M. Courtemanche, R. J. Ramirez, and S. Nattel, Am. J Physiol. **275**, H301 (1998).
[6]F. Fenton and A. Karma, Chaos **8**, 20 (1998).
[7]F. H. Fenton, E. M. Cherry, H. M. Hastings, and S. J. Evans, Chaos **12**, 852 (2002).
[8]E. Grandi, S. V. Pandit, N. Voigt, A. J. Workman, D. Dobrev, J. Jalife, and D. M. Bers, Circ. Res. **109**, 1055 (2011).
[9]C. M. Gray, A. K. Engel, P. König, and W. Singer, Visual Neurosci. **8**, 337 (1992).
[10]R. Gray, A. Pertsov, and J. Jalife, Nature **392**, 75 (1998).
[11]R. N. Gutenkunst, J. J. Waterfall, F. P. Casey, K. S. Brown, C. R. Myers, and J. P. Sethna, PLoS Comput. Biol. **3**, e189 (2007).
[12]M. Haissaguerre, M. Hocini, A. Denis, A. J. Shah, Y. Komatsu, S. Yamashita, M. Daly, S. Amraoui, S. Zellerhoff, M. Q. Picat, A. Quotb, L. Jesel, H. Lim, S. Ploux, P. Bordachar, G. Attuel, V. Meillet, P. Ritter, N. Derval, F. Sacher, O. Bernus, H. Cochet, P. Jais, and R. Dubois, Circulation **130**, 530 (2014).
[13]J. Jalife, Cardiovasc. Res. **89**, 766 (2011).
[14]A. Karma, Annu. Rev. Condens. Matter Phys. **4**, 313 (2013).
[15]B. Y. Kogan, W. J. Karplus, B. S. Billett, A. T. Pang, H. S. Karagueuzian, and S. S. Khan, Phys. D: Nonlinear Phenom. **50**, 327 (1991).
[16]J. T. Koivumaki, T. Korhonen, and P. Tavi, PLoS Comput. Biol. **7**, e1001067 (2011).
[17]J. T. Koivumaki, G. Seemann, M. M. Maleckar, and P. Tavi, PLoS Comput. Biol. **10**, e1003620 (2014).
[18]D. M. Lombardo, F. H. Fenton, S. M. Narayan, and W.-J. Rappel, PLoS Comput. Biol. **12**, e1005060 (2016).
[19]M. M. Maleckar, J. L. Greenstein, N. A. Trayanova, and W. R. Giles, Prog. Biophys. Mol. Biol. **98**, 161 (2008).
[20]K. S. McDowell, F. Vadakkumpadan, R. Blake, J. Blauer, G. Plank, R. S. MacLeod, and N. A. Trayanova, J. Electrocardiol. **45**, 640 (2012).
[21]S. M. Narayan, D. E. Krummen, M. W. Enyeart, and W.-J. Rappel, PLoS One **7**, e46034 (2012).
[22]S. M. Narayan, D. E. Krummen, and W. Rappel, J. Cardiovasc. Electrophysiol. **23**, 447 (2012).
[23]S. M. Narayan, D. E. Krummen, K. Shivkumar, P. Clopton, W.-J. Rappel, and J. M. Miller, J. Am. Coll. Cardiol. **60**, 628 (2012).
[24]A. Nygren, C. Fiset, L. Firek, J. W. Clark, D. S. Lindblad, R. B. Clark, and W. R. Giles, Circ. Res. **82**, 63 (1998).
[25]Z. Qu, F. Xie, A. Garfinkel, and J. N. Weiss, Ann. Biomed. Eng. **28**, 755 (2000).
[26]W.-J. Rappel, Chaos **11**, 71 (2001).
[27]M. K. Transtrum, B. B. Machta, and J. P. Sethna, Phys. Rev. Lett. **104**, 060201 (2010).
[28]M. K. Transtrum and P. Qiu, Phys. Rev. Lett. **113**, 098701 (2014).
[29]N. A. Trayanova, IEEE Spectrum **51**, 34 (2014).
[30]K. H. ten Tusscher and A. V. Panfilov, Am. J. Physiol.-Heart Circ. Physiol. **291**, H1088 (2006).
[31]N. Virag, V. Jacquemet, C. Henriquez, S. Zozor, O. Blanc, J.-M. Vesin, E. Pruvot, and L. Kappenberger, Chaos **12**, 754 (2002).
[32]M. Wilhelms, H. Hettmann, M. M. Maleckar, J. T. Koivumaki, O. Dossel, and G. Seemann, Front Physiol. **3**, 487 (2012).
[33]M. Zoni-Berisso, F. Lercari, T. Carazza, S. Domenicucci *et al.*, Clin. Epidemiol. **6**, e220 (2014).